DOI: 10.1002/ejic.200900145

Mild Hydrothermal Synthesis and Structural Determination of Two Layered, Structurally Related Inorganic–Organic Hybrid Vanadates with Nickel(II) and Tris(2-aminoethyl)amine

Edurne S. Larrea,[a] José L. Mesa,*[a] José L. Pizarro,[b] Jesús Rodríguez-Fernández,[c] María I. Arriortua,[b] and Teófilo Rojo[a]

Keywords: Hydrothermal synthesis / X-ray diffraction / Thermochemistry / UV/Vis spectroscopy / Magnetic properties

2D $Ni_2(C_6H_{19}N_4)_2(V_6O_{18})\cdot 2H_2O$ (**1**) and $Ni_2(C_6H_{19}N_4)_2(V_6O_{18})\cdot H_2O$ (**2**) are inorganic–organic hybrid compounds that have been synthesised under hydrothermal conditions. Crystalline aggregates composed of both compounds were obtained and structural characterisation was subsequently carried out using single crystalline fragments of these aggregates. Optimisation of the synthetic conditions allowed us to obtain **1** as a polycrystalline powder. The crystal structures of **1** and **2** were solved using single-crystal X-ray diffraction data. Both compounds are structurally related, as the layers from which they are built have the same composition and connectivity in both structures. The main differences between them are the layer stacking and water contents. UV/Vis spectroscopy of **1** shows the characteristic features of the Ni^{II} d^8 cation in slightly distorted octahedral symmetry. From the temperature-dependent magnetic susceptibility measurements the parameter $D/hc = -3.75\ cm^{-1}$ was obtained. Phase **1** undergoes a reversible structural transformation at approximately 60 °C as a result of the dehydration process. This dehydration gives rise to a decrease in the unit cell volume.

Introduction

During the last decades the chemistry of vanadium has enjoyed great developments due to the potential applications of vanadium derivatives. Specifically, there has been much interest in layered vanadium oxides and their intercalates because of their potential use as secondary cathode materials for advanced lithium batteries.[1] As a result, the rich crystal chemistry of the vanadates has increased significantly.

Interest in vanadium derivatives stems from the variety of oxidation states that this metal can exhibit. Each oxidation state can show different coordination polyhedra, ranging from the ideal octahedron for the oxidation state three to the tetrahedron for the oxidation state five, going through the distorted octahedron, the square-based pyramid and the trigonal bipyramid (oxidation states four and five).[2] In addition, vanadium polyhedra have a great ability to polymerise, giving rise to clusters, rings, chains, layers and 3D frameworks.[3] The polymer grade is closely related to the synthetic conditions and, in particular, the pH during the reaction.[4]

The microstructures of vanadium oxides can be influenced by the introduction of organic molecules in the structures. The organic constituent may adopt a variety of roles ranging from charge compensator to a ligand for the secondary metal.[5] Vanadium/transition metal/organic molecular systems in which the organic molecule acts as a ligand for the transition metal that is linked to the $[V_xO_n]^{-y}$ skeleton through oxido bridging groups have been studied.[6] In these kinds of hybrid compounds, considerable structural versatility is achieved. Of note is the existence of the $[M(Hdpa)_2V_4O_{12}]$ (Hdpa; 4,4′-dipyridylamina; M; Co or Ni) phases, with 2D structures constructed from bimetallic oxide networks $\{MV_4O_{12}\}_n^{2n-}$ with monodentate Hdpa projecting from the protonated ring into the interlamellar region.[7a] The hydrothermal reactions of the V_2O_5/2,2′:6′,2′′-terpyridine/ZnO/H_2O system under a variety of conditions yielded the organic–inorganic hybrid materials $[V_2O_4(terpy)_2]_3[V_{10}O_{28}]\cdot 2H_2O$, $[VO_2(terpy)][V_4O_{10}]$ and $[V_9O_{22}(terpy)_3]$, which exhibit different crystal structures containing discrete binuclear cations $[V_2O_4(terpy)_2]^{2+}$ to discrete mononuclear cations $[VO_2(terpy)]^+$ and linear $\{V_3O_5(terpy)_3\}$ moieties of corner-sharing vanadium octahedra.[7b] Vanadium oxides with other transition elements are also known. In this way, Cu^{II} compounds with formulae

[a] Dpto. Química Inorgánica, Universidad del País Vasco (UPV/EHU),
Apdo. 644, 48080 Bilbao, Spain
E-mail: joseluis.mesa@ehu.es
[b] Dpto. Mineralogía y Petrología, Universidad del País Vasco (UPV/EHU)
Apdo. 644, 48080, Bilbao, Spain
[c] Dpto. CITIMAC, Facultad de Ciencias, Universidad de Cantabria,
39005 Santander, Spain

Supporting information for this article is available on the WWW under http://dx.doi.org/10.1002/ejic.200900145.

[Cu(2,2′-bipyridine)V_2O_6] and β-[Cu(2,2′:6′,2′′-terpyridine)-V_2O_6][7c] and the Zn^{II} and Cu^{II} phases with tpytrz {2,4,6-tri(4-pyridyl)-1,3,5-trizine},[$Zn(tpytrz)_2V_2O_6$],[$Zn_3(tpytrz)_2$-$(H_2O)_2V_6O_{18}$]·$6H_2O$ and [$Cu_3(tpytrz)_2(H_2O)_2$ $V8O_{23}$]·$3H_2O$ have been prepared.[7d] Finally, a large number of VO/Ni-ethylenediamine systems where the aliphatic organic molecule is bidentate has been synthesised and studied.[8]

In our previous work, we used aromatic diamines with nitrogen atoms in relative positions such as 4,4′-bipyridine or 1,2-bis(4-pyridyl)ethylene or pyrazine[9–11] as ligands that favour the bridging between the metal centres. In this work we present the results obtained for the vanadium/nickel(II)/tris(2-aminoethyl)amine system in which the aliphatic amine has its nitrogen atoms in an appropriate position to chelate the nickel(II) atoms. We here describe the mild hydrothermal synthesis of two inorganic–organic hybrid vanadates with nickel(II) as the transition metal and tris(2-aminoethyl)amine as the organic ligand, namely, $Ni_2(C_6H_{19}N_4)_2$-(V_6O_{18})·$2H_2O$ (**1**) and $Ni_2(C_6H_{19}N_4)_2(V_6O_{18})$·$H_2O$ (**2**). The structural characterisation of both phases and the thermal, spectroscopic and magnetic studies of compound **1** are also reported.

Results and Discussion

Hydrothermal Synthesis of $Ni_2(C_6H_{19}N_4)_2(V_6O_{18})$·$2H_2O$ (1) and $Ni_2(C_6H_{19}N_4)_2(V_6O_{18})$·$H_2O$ (2)

Attempts at synthesis using different pH values were made by using equimolar amounts (0.86 mmol) of $Ni(NO_3)_2$·$6H_2O$, $NaVO_3$ and tris(2-aminoethyl)amine (Tae). The pH was modified with a 1 M hydrochloric acid solution. After maintaining the reactions for 2 d at 120 °C in an oven, compound **1** was obtained at pH 6 as a polycrystalline green powder.

In order to obtain this product as single-crystals, some of the reaction conditions such as temperature, total concentration and relative amounts of the reagents were modified. After several attempts under different conditions, crystalline aggregates were obtained. These aggregates, green in colour and planar in form, were composed of two different types of crystals of compounds **1** and **2**.

Several attempts with different synthetic conditions were made in order to obtain both compounds as pure phases. In this stage, we observed that when the synthetic conditions favour the growth of the crystals, they grew together forming aggregates and, with fast crystallisation conditions, polycrystalline powders of **1** were obtained. Hence, the crystal structures of both compounds were solved using fragments of these crystalline aggregates. In order to corroborate the purity of **1**, its powder diffraction pattern was refined using the Rietveld procedure (see Supporting Information).

Crystal Structure of $Ni_2(C_6H_{19}N_4)_2(V_6O_{18})$·$2H_2O$ (1) and $Ni_2(C_6H_{19}N_4)_2(V_6O_{18})$·$H_2O$ (2)

Both compounds exhibit 2D structures formed by (001) layers (Figure 1). The composition and connectivity in these layers is the same for **1** and **2**, the main difference between **1** and **2** being the layer stacking (Figure 2). An ORTEP drawing of **1** and **2** with details of the labelling of the atoms is given in Figure 3.

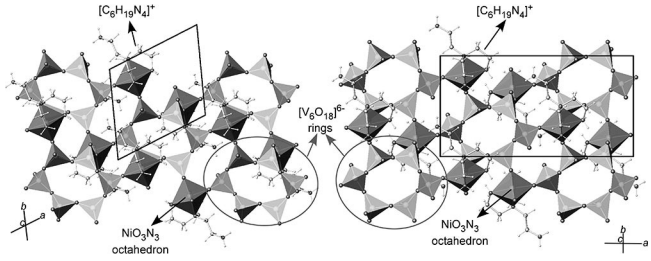

Figure 1. Polyhedral view of the layers present in **1** and **2**.

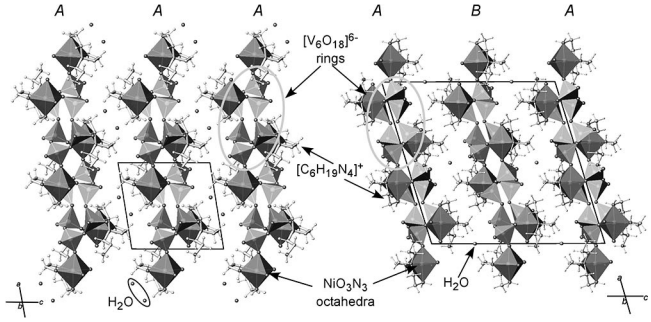

Figure 2. Polyhedral view of the layer stacking in phases **1** and **2**.

The layers in **1** and **2** are constructed from VO_4 tetrahedra and NiO_3N_3 octahedra. The VO_4 tetrahedra are linked by vertices giving rise to six-membered $[V_6O_{18}]^{6-}$ rings. Each tetrahedron shares one oxygen atom with a nickel(II) octahedron. Thus, each NiO_3N_3 octahedron is linked to three different $[V_6O_{18}]^{6-}$ rings. The oxygen atoms are located on one face of the NiO_3N_3 octahedron and the vertices of the opposite face are occupied by three nitrogen atoms of the organic molecule Tae. The uncoordinated nitrogen atom of Tae is protonated (see Figure 1).

The stacking of the layers in both compounds is parallel to (100). However, whereas in compound **1** the sequence is A A A, in compound **2** it is A B A, where A and B are related by a binary rotation axis. This difference in the stacking results in the slight differences observed in the layers (see Figure 2).

Another difference is the amount of water that can be placed between the layers. In compound **1** there is one water molecule per nickel atom, whereas in compound **2** there is half a water molecule per nickel atom. This structural similarity between compounds **1** and **2**, together with the difficulties in obtaining them as unique products, suggests that the energetic difference between **1** and **2** is small.

The Ni–O and Ni–N bond lengths range from 2.069(3) to 2.164(3) Å for phase **1** and from 2.029(2) to 2.133(3) Å for phase **2**. In phase **1** the *cis* angles are between 97.5(1) and 82.8(1)° and the *trans* angles are between 176.0(1) and 173.6(1)°. In phase **2** these angles range from 98.3(1) to 83.2(1)° and from 177.5(1) to 172.7(1)°, respectively.

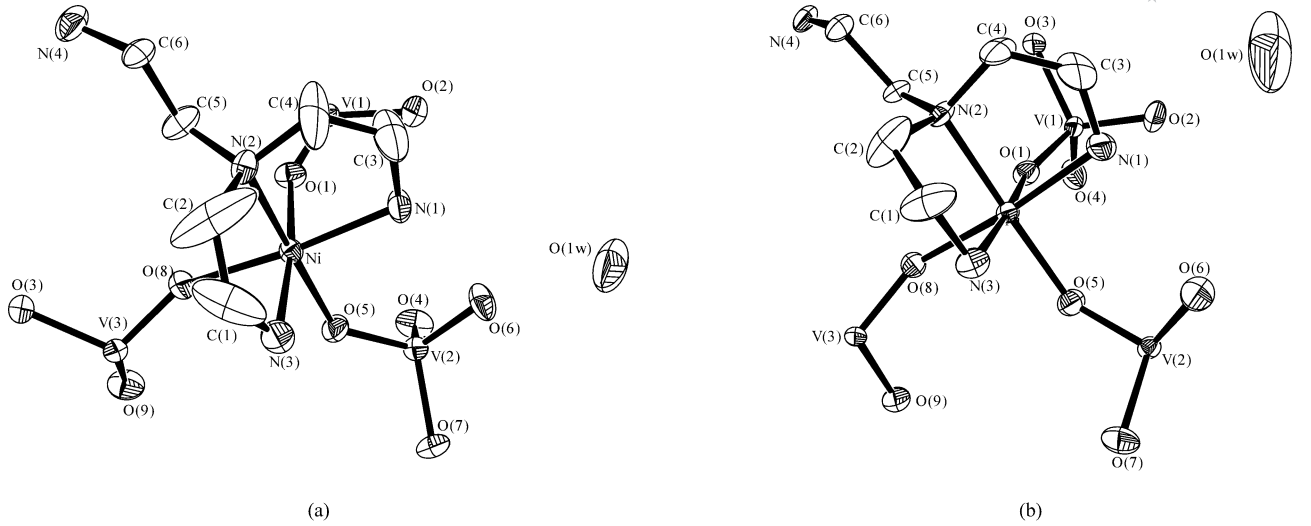

Figure 3. ORTEP drawing with details of the labelling of the atoms for the asymmetric units of (a) $Ni_2(C_6H_{19}N_4)_2(V_6O_{18})\cdot 2H_2O$ (**1**) and (b) $Ni_2(C_6H_{19}N_4)_2(V_6O_{18})\cdot H_2O$ (**2**).

The vanadium(V) tetrahedra have different V–O bond lengths depending on the connectivity of the oxygen atom. The V=O terminal bond lengths in both phases are slightly longer than expected because the oxygen atoms form part of a hydrogen bond. These distances are approximately 1.63 Å. The V–O bonds in which the oxygen atom is linked to a nickel(II) atom are in the range from 1.64 to 1.65 Å in both phases. Finally, the V–O bonds, the oxygen of which is linked to another vanadium(V) atom, are between 1.78 and 1.80 Å. The tetrahedra bond angles vary between 106.2(1) and 116.6(1)° for compound **1** and between 106.2(1) and 112.1(1)° for compound **2**.

Hydrogen bonds are established between the hydrogen atoms of the amine groups and the oxygen atoms from the same layer. In phase **1**, two of these hydrogen bonds are established with the oxygen atom of the water molecule, N(1)–H(1)···O(1w) and N(3)–H(4)···O(1w). The position of the hydrogen of the water molecules involved in the hydrogen bonds could not be calculated.

The distortion of the different polyhedra present in the structures of **1** and **2** has been evaluated using continuous symmetry measure (CSM)[12] based on the comparison of the real polyhedron and the ideal polyhedron most resembling the real one. These calculations were carried out with the Shape v1.1a program, developed by Alvarez et al.[13] The NiO_3N_3 octahedra of phases **1** and **2** have very similar distortions. The $S(O_h)$ value for the octahedra present in phase **1** is 0.42 and for phase **2** it is 0.44, indicating small distortions. The $S(T_d)$ values calculated for the VO_4 tetrahedra of both phases range from 0.16 to 0.23 for **1** and from 0.17 to 0.23 for **2**. These values indicate that the vanadium(V) environment is very regular.[14,15]

Thermal Analysis

A thermal analysis was carried out for compound **1**. The thermogravimetric curve shows two mass loss processes. The first takes place between 43 and 80 °C and is an endothermic process according to the DTA curve. The corresponding mass loss is 3.4% which is in good agreement with the water content of compound **1**. Above 240 °C, the second mass loss process starts. This process overlaps with successive steps up to 485 °C. All of these overlapping processes are exothermic and the total mass lost corresponds to 31%. In this temperature range the calcination of the organic molecule Tae takes place representing 28.3% of the mass of the compound. The difference between the theoretical and the observed percentage may be due to the reorganisation of the remaining inorganic moieties. The obtained residue was analysed by powder X ray diffraction and it consists of a mixture of vanadium(V) oxide V_2O_5 [$Pmn2_1$, a = 11.503 Å, b = 4.369 Å, c = 3.557 Å][16] and nickel(II) vanadate NiV_2O_6 [$P1$, a = 7.128 Å, b = 8.820 Å, c = 4.793 Å, α = 90.24°, β = 94.10°, γ = 102.15°].[17]

Thermodiffractometric analysis revealed that the dehydration of compound **1** involves a reversible structural transformation that occurs at approximately 60 °C (see Figure 4). This dehydrated phase is stable until 260 °C giving rise to an amorphous phase that at 430 °C gives rise to the same residue obtained in the thermogravimetric process.

When phase **1** is heated up to 70 °C the dehydration process takes place but when the temperature goes down the compound absorbs water from the atmosphere turning back to **1** again. This dehydration–hydration process involves a hysteresis loop of 20 °C (Figure 5). The dehydration also takes place when **1** is exposed to a vacuum of 10^{-3} bar, indicating that the water molecules are not strongly linked.

The X-ray powder diffraction pattern of the dehydrated phase was analysed. The diffraction maxima were indexed with the DICVOL04[18] program. A triclinic unit cell was obtained with cell parameters a = 10.543(1) Å, b = 9.441(1) Å, c = 9.776(1) Å, α = 101.77(1)°, β = 107.95(1)°, γ = 63.53(1)° and V = 822.71 Å^3 with figures of merit $M(20)$

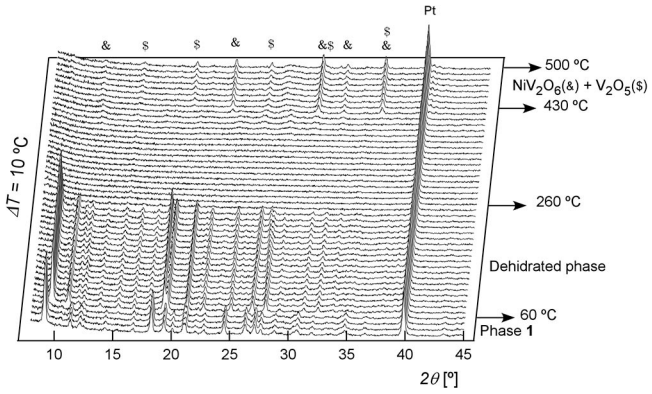

Figure 4. Thermodiffractogram of compound **1**.

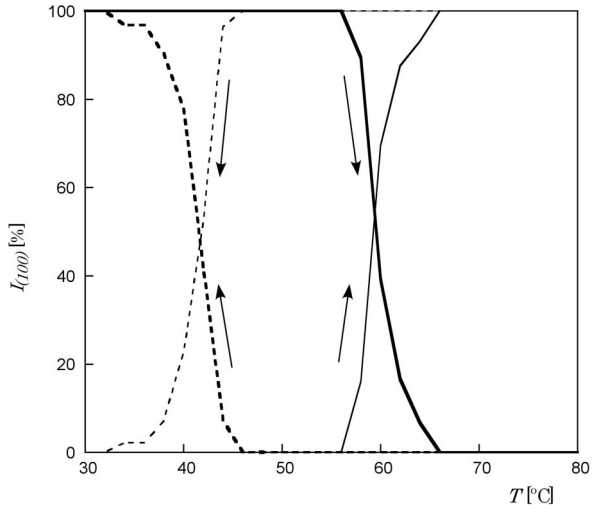

Figure 5. Evolution of the intensity of the (001) diffraction maximum of the hydrated phase **1** (thick line) and the dehydrated phase (thin line) when the temperature was increased (continuous line) and when it was decreased (broken line).

= 18.8 and $F(20) = 37.0$. The cell volume is reduced from 860.78 to 822.71 Å^3 in good agreement with the elimination of the interlayer water molecules. Comparing the cell parameters with those of the hydrated phase we can conclude that the elimination of the water molecules causes the approach of the layers. When dehydration takes place, the layers in the structure of **1** move closer and a slight reorganisation occurs within them. The approach of the layers results in the reduction of the reticular space in (001) from 9.59 Å for **1** to 9.00 Å for the dehydrated phase and, consequently, a decrease in the parameter *c*. The variation of the rest of the cell parameters could be attributed to the adaptation of the layers when the water molecules are removed.

UV/Vis Spectroscopy

In the UV/Vis spectrum of **1**, two absorption bands corresponding to the allowed transitions $^3A_{2g}(^3F) \rightarrow {}^3T_{2g}(^3F)$ at 9700 cm^{-1} and $^3A_{2g}(^3F) \rightarrow {}^3T_{1g}(^3F)$ at 16000 cm^{-1} can be observed. Another band appears as a shoulder overlapping the first band at 12200 cm^{-1} due the forbidden transition $^3A_{2g}(^3F) \rightarrow {}^1E_g(^1D)$. The values of the crystal field splitting and the Racah parameters *B* and *C* were calculated by fitting the experimental frequencies to an energy level diagram for octahedral d^8 systems,[19] $Dq = 970$ cm^{-1}, $B = 980$ cm^{-1}, 95% of the Ni^{II} free ion and $C = 2485$ cm^{-1}. These values are in good agreement with those usually found for octahedral Ni^{II} compounds.[20,21]

Magnetic Behaviour

The χ vs. *T* curve for compound **1**, recorded at a magnetic field of 0.1 T, increases with decreasing temperature over the entire temperature range. This behaviour is typical of a paramagnetic compound with hexacoordinate Ni^{II} ions ($S = 1$) with zero-field splitting in the ground state. This zero-field splitting effect was expected because the minimum distance between two Ni^{II} ions, at 6.2 Å, is too large for direct interactions between the metallic centres. The thermal evolution of $1/\chi_m$ follows the Curie–Weiss law over the entire temperature range with Curie and Weiss parameters $C_m = 1.16$ cm^3 K mol^{-1} and $\theta = -1.13$ K, respectively. Taking into account these results the thermal evolution of χ_m was fitted with the ZFS equation [Equation (1)].[22]

$$\langle\chi\rangle = \frac{2Ng^2\beta^2}{3kT}\left[\frac{2/x - 2\exp(-x)/x + \exp(-x)}{1 + 2\exp(-x)}\right] \quad (1)$$

where $x = D/kT$

The best fitting parameters obtained were $g = 2.16$ and $D/hc = -3.75$ cm^{-1} ($R = 0.9991$). The *D* parameter value is consistent with the presence of light distorted octahedra.[23]

Conclusions

$Ni_2(C_6H_{19}N_4)_2(V_6O_{18})\cdot 2H_2O$ (**1**) and $Ni_2(C_6H_{19}N_4)_2(V_6O_{18})\cdot H_2O$ (**2**) were hydrothermally synthesised as crystalline aggregates. Both phases are structurally related, exhibiting a 2D structure composed of (001) layers with the same composition and connectivity. Phase **1** was obtained as a chemically pure compound and suffers a reversible structural transformation approximately at 60 °C, giving rise to a dehydrated compound with a similar layered structure. The UV/Vis spectrum is typical of a slightly distorted Ni^{II} d^8 octahedron. The magnetic behaviour shows a zero-field splitting of the ground state characteristic of noninteracting Ni^{II} centres.

Experimental Section

Physical Measurements: The IR spectrum (KBr pellets) of **1** was obtained with a Jasco FT-R 6100 spectrometer in the 400–4000 cm^{-1} range. The UV/Vis spectrum of the powdered sample of **1** (diffuse reflectance) was registered at room temperature with a Varian Cary 5000 spectrometer in the 200–2500 nm range. Thermogravimetric analysis (TGA) was performed under synthetic air in a DSC simultaneous differential scanning calorimetry (DSC)-TGA TA instrument. A crucible containing approximately 8 mg of the

sample was heated at 5 °C min^{-1} in the temperature range 30–500 °C. Thermodiffractometric analysis was performed with a Bruker D8 Advance Vantec diffractometer equipped with an Anton Parr HTK2000 variable temperature stage with a Pt sample holder. The diffraction patterns were collected in 2θ steps of 0.01667° in the range of 8–45°, counting for 0.1 s per step and increasing the temperature at 10 °C min^{-1} from room temperature up to 500 °C. Magnetic measurements were performed on a Quantum Design MPMS-7 SQUID magnetometer. The magnetic susceptibility data were obtained from the powdered sample in the temperature range 2.0–300 K at different magnetic fields, first after zero-field cooling (ZFC) and next after field cooling (FC).

Synthesis and Characterisation: $Ni_2(C_6H_{19}N_4)_2(V_6O_{18})\cdot 2H_2O$ (**1**) was synthesised using mild hydrothermal conditions employing PTFE reactors. In the synthesis of **1**, $Ni(NO_3)_2\cdot 6H_2O$ (100 mg, 0.34 mmol) and $NaVO_3$ (41.93 mg, 0.34 mmol) were dissolved in distilled water (30 mL) and Tae (53.6 μL, 0.34 mmol) was added. The mixture was stirred in a PTFE reactor. The pH was adjusted to 6 by adding 1 M hydrochloric acid solution. The reactor was placed in an oven at 120 °C for 3 d and was then cooled to room temperature at a rate of 1 °C min^{-1}. The resultant product, a green powder, was filtered and washed with distilled water and acetone and left to air dry.

Crystalline aggregates of both compounds, **1** and **2**, green and planar, were obtained when a mixture of $Ni(NO_3)_2\cdot 6H_2O$ (100 mg, 0.34 mmol), $NaVO_3$ (88.86 mg, 0.68 mmol) and Tae (53.6 μL) in distilled water (30 mL), with a pH of 7, was heated in a PTFE reactor at 120 °C for 3 d. The obtained green crystalline aggregates were isolated and left to air dry.

The amounts of nickel and vanadium in compound **1** were measured by inductively coupled plasma atomic emission spectroscopy and C, N and H contents were determined by elemental analysis. $Ni_2(C_6H_{19}N_4)_2(V_6O_{18})\cdot 2H_2O$ (**1**) (1041.6): calcd. C 13.82, H 4.13, N 10.75, Ni 11.27, V 29.28; found C 13.63(30), H 4.17(50), N 10.84(20), Ni 11.12(10), V 29.02(20). The density of **1** was measured by a flotation method,[24] using a mixture of CH_2I_2 and CH_2Cl_2 and was found to be 1.98(2) g cm^{-3}.

The IR spectrum of **1** shows the following bands: stretching vibrations, ν(O–H), of water at 3440 and 3330 cm^{-1} and δ(O–H) at 1640 cm^{-1}. Between 3300 and 2400 cm^{-1} the ν(C–H) and ν(N–H) bands of Tae appear. The bands between 1500 and 1240 cm^{-1} can be attributed to its bending vibrations. The vibrations of the N–H bonds in the protonated amines appear at 1590 cm^{-1}. Between 1500 and 1240 cm^{-1} the ν(C–C) and ν(C–N) bands can be observed. The band occurring at 950 cm^{-1} is caused by the ν_s(V=O) mode. The bands at 920 and 750 cm^{-1} are the ν_{as}(V–O) mode, the first band corresponding to V–O–V and the second to the V–O–Ni bond. The bands at 682, 640, 510 and 560 cm^{-1} are related to the ν_s(V–O–V) and ν_s(V–O–Ni) modes.[25]

Crystal X-ray Diffraction: From a sample of the crystalline aggregates of **1** and **2**, two single-crystalline pieces of both phases were selected under a polarising microscope and glued onto glass fibres. Diffraction data were collected with an Oxford Diffraction Xcalibur2 diffractometer using graphite monochromated Mo-K_α radiation (λ = 0.71073 Å) at 293(2) K. Details of crystal data, intensity collection and some features of the structural refinement are reported in Table 1. A total of 5577 and 7889 reflections for **1** and **2**, respectively, were measured in the ranges $2.50 \le 2\theta \le 26.50°$ and $2.52 \le 2\theta \le 26.50°$, respectively. The independent reflections were 3313 (R_{int} = 0.0540) for **1** and 3343 (R_{int} = 0.0432) for **2**, observed applying the criterion $I > 2\sigma(I)$. The diffraction data were corrected for Lorentz and polarisation effects[26] as well as for the absorption, taking into account the crystals shape and size. The structures were solved by direct methods (SHELXS97[27]) and refined by the full-matrix least-squares procedure based on F^2, using the SHELXL 97[28] computer program belonging to the WINGX software package.[29] The asymmetric units of both structures are shown in Figure 3 as an ORTEP drawing. Scattering factors were taken from ref.[29] Anisotropic thermal parameters were used for all atoms except for the hydrogen atoms of the organic molecule which were

Table 1. Details of the crystal data, structural resolution and refinement procedure for compounds **1** and **2**.

	1	**2**
Empirical Formula	$C_6H_{21}N_4NiO_{10}V_3$	$C_{12}H_{40}N_8Ni_2O_{19}V_6$
Formula Weight [g mol^{-1}]	520.80	1023.58
Crystal system, space group	triclinic, $P\bar{1}$	monoclinic, $C2/c$
a [Å]	10.2239(5)	19.065(1)
b [Å]	9.5116(4)	9.456(1)
c [Å]	10.2507(6)	19.601(1)
α [°]	106.253(4)	90
β [°]	104.723(5)	107.119(4)
γ [°]	65.642(4)	90
V [Å^3], Z	860.78(7), 2	3377.1(4), 4
$\rho_{obsd.}$, $\rho_{calcd.}$ [g cm^{-3}]	1.98(2), 2.009	–, 2.013
F(000)	524	2056
μ [mm^{-1}]	2.708	2.757
Colour, morphology	green, planar	green, planar
Crystal size [mm]	0.11 × 0.06 × 0.04	0.30 × 0.13 × 0.03
θ range [°]	2.50–26.50	2.52–26.50
Limiting indices	±12, $-9 \le h \le 11$, ±12	$-22 \le h \le 23$, ±11; $-24 \le k \le 22$
Reflections collected / unique	5577 / 3313	7889 / 3343
R_{int}	0.0540	0.0432
Data / Restrains / Parameters	3313 / 0 / 219	3343 / 0 / 215
Final R indices [$I > 2\sigma(I)$]	R_1 = 0.0449, wR_2 = 0.0645	R_1 = 0.0334, wR_2 = 0.0548
R indices [all data]	R_1 = 0.0918, wR_2 = 0.0707	R_1 = 0.0670, wR_2 = 0.0588
$w = 1/[\sigma^2\|F_o\|^2+(xp)^2+yp]$, $p = [\max\|F_o\|^2+2\|F_c\|^2]/3$	x = 0.0187, y = 0	x = 0.015, y = 0
Largest diff. peak and hole [e Å^{-3}]	0.563, –0.542	0.819, –0.890
GOF	0.917	0.924

located geometrically and refined with common isotropic displacements. In both structures, oxygen atoms belonging to water molecules exhibit large thermal ellipsoids due to the high mobility of the water molecules in the structure. This fact is in good agreement with this facility of the molecules to be removed from the interlayer space. It is also noteworthy that the thermal parameters of the carbon atoms C(1), C(2), C(3) and C(4) [belonging to the branches of the Tae molecule bonded to nickel(II) atom] are rather high. Splitting the location of these atoms in two different nearby positions using a disorder scheme, did not result in a better agreement factor. Hence, we considered them in a single position. Final *R* factors are $R_1 = 0.0449$, and $wR_2 = 0.0645$, and $R_1 = 0.0334$ and $wR_2 = 0.0548$ for **1** and **2**, respectively. Maximum and minimum peaks in the final synthesis difference maps were 0.561 and –0.518 for **1**, and 0.800 and –0.875 e Å^{-3} for **2**. Selected bond lengths and angles are included in the Supporting Information. CCDC-718965 (for **1**) and -718966 (for **2**) contain the supplementary crystallographic data for this paper. These data can be obtained free of charge from The Cambridge Crystallographic Data Centre via www.ccdc.cam.ac.uk/data_request/cif.

Supporting Information (see footnote on the first page of this article): Selected bond lengths and angles for structures **1** and **2**, magnetic measurement curves and Rietveld refinement of **1**.

Acknowledgments

This work has been financially supported by the Ministerio de Educación y Ciencia (MAT2007-60400, MAT2007-66737-C02-01) and the Gobierno Vasco (IT-177–07, IT-312-07). The authors thank the technicians of the Servicios Generales de Investigación [SGiker], financed by the National Program for the Promotion of Human Resources within the National Plan of Scientific Research, Development and Innovation, Ministerio de Educación y Ciencia and Fondo Social Europeo for the measurements carried out. E S. L. thanks the Universidad del Pais Vasco/Euskal Herriko Unibertsitatea [UPV/EHU] for funding.

[1] M. S. Whittingham, *J. Electrochem. Soc.* **1976**, *123*, 315–320; W. Li, J. R. Dahn, D. S. Wainwright, *Science* **1994**, *264*, 1115–1118.
[2] M. Schindler, F. C. Hawthorne, W. H. Baur, *Chem. Mater.* **2000**, *12*, 1248–1259.
[3] P. Y. Zavalij, M. S. Whittingham, *Acta Crystallogr., Sect. B* **1999**, *55*, 627–663.
[4] M. Schindler, F. C. Hawthorne, W. H. Baur, *Can. Mineral.* **2000**, *38*, 1443–1456; J. Livage, *Coord. Chem. Rev.* **1998**, *178–180*, 999–1018.
[5] P. J. Hagrman, R. C. Finn, J. Zubieta, *Solid State Sci.* **2001**, *3*, 745–774.
[6] a) Z.-H. Yi, X.-B. Cui, X. Zhang, J.-H. Yu, J. Lu, J.-Q. Xu, G.-D. Yang, T.-G. Wang, H.-H. Yu, W.-J. Duan, *Dalton Trans.* **2007**, *21*, 2115–2120; b) T. S. C. Law, I. D. Williams, *Chem. Mater.* **2000**, *12*, 2070–2072; c) L. M. Zheng, J. S. Zhao, K. H. Lii, L. Y. Zhang, Y. Liu, X. Q. Xin, *J. Chem. Soc., Dalton Trans.* **1999**, *6*, 939–944; d) Y. Zhang, J. R. D. DeBord, C. J. O'Connor, R. C. Haushalter, A. Clearfield, J. Zubieta, *Angew. Chem. Int. Ed. Engl.* **1996**, *35*, 989–991.
[7] a) R. L. LaDuca, R. S. Rarig, J. Zubieta, *Inorg. Chem.* **2001**, *40*, 607–612; b) P. J. Hagrman, J. Zubieta, *Inorg. Chem.* **2000**, *39*, 3252–3260; c) R. C. Finn, J. Sims, C. J. O'Connor, J. Zubieta, *J. Chem. Soc., Dalton Trans.* **2002**, *2*, 159–163; d) R. S. Rarig, J. Zubieta, *Dalton Trans.* **2003**, *9*, 1861–1868.
[8] a) S.-X. Liu, B.-Z. Lin, S. Lin, *Inorg. Chim. Acta* **2000**, *304*, 33–37; b) Z. Shi, L. Zhang, G. Zhu, G. Yang, J. Hua, H. Ding, S. Feng, *Chem. Mater.* **1999**, *11*, 3565–3570; c) P. Y. Zavalig, F. Zhang, M. S. Whittingham, *Acta Crystallogr., Sect. B* **1999**, *55*, 953–962; d) Y.-B. Liu, J.-H. Yu, J. Liu, Y.-K. Lu, J.-Q. Xu, T.-G. Wang, *J. Mol. Struct.* **2007**, *833*, 58–64.
[9] E. S. Larrea, J. L. Mesa, J. L. Pizarro, M. I. Arriortua, T. Rojo, *J. Solid State Chem.* **2007**, *180*, 1149–1157.
[10] R. Fernández de Luis, J. L. Mesa, M. K. Urtiaga, L. Lezama, M. I. Arriortua, T. Rojo, *New J. Chem.* **2008**, *32*, 1582–1589.
[11] R. Fernández de Luis, M. K. Urtiaga, J. L. Mesa, T. Rojo, M. I. Arriortua, *J. Alloys Compd.* **2008**, DOI: 10.1016/j.jallcom.2008.09.182.
[12] a) H. Zabrodsky, S. Peles, D. Avnir, *J. Am. Chem. Soc.* **1992**, *114*, 7843–7851; b) M. Prinsky, D. Avnir, *Inorg. Chem.* **1998**, *37*, 5575–5582.
[13] M. Llunel, D. Casanova, J. Cirera, J. M. Bofill, P. Alemany, S. Álvarez, M. Pinsky, D. Yatunir, *SHAPE (v1.1a): Program for Continuous Shape Measure Calculations of Polyhedral Xn and MLn Fragments*, **2003**.
[14] S. Alvarez, D. Avnir, M. Llunell, M. Pinsky, *New J. Chem.* **2002**, *26*, 996–1009.
[15] J. Cirera, P. Alemany, S. Alvarez, *Chem. Eur. J.* **2004**, *10*, 190–207.
[16] *"Powder Diffraction File - Inorganic and Organic"*, ICCD, Pennsylvania. File 86–2248, **2001**.
[17] *"Powder Diffraction File - Inorganic and Organic"*, ICCD, Pennsylvania. File 76–0359, **2001**.
[18] A. Boufil, D. Louer, *J. Appl. Crystallogr.* **2004**, *37*, 724–731.
[19] a) Y. Tanabe, S. Sugano, *J. Phys. Soc. Jpn.* **1954**, *9*, 753–766; b) Y. Tanabe, S. Sugano, *J. Phys. Soc. Jpn.* **1954**, *9*, 766–779.
[20] A. B. P. Lever, *Inorganic Electronic Spectroscopy*, Elsevier, Amsterdam, **1984**.
[21] J. Escobal, J. L. Pizarro, J. L. Mesa, M. I. Arriortua, T. Rojo, *J. Solid State Chem.* **2000**, *154*, 460–465.
[22] R. L. Carlin, *Magnetochemistry*, Springer, Berlin, **1986**, ch. 2, pp. 19–34.
[23] a) J. Titiš, R. Boča, L′. Dlháň, T. Ďurčeková, H. Fuess, R. Ivaniková, V. Mrázová, B. Papánková, I. Svoboda, *Polyhedron* **2007**, *26*, 1523–1530; b) R. Ivaniková, R. Boča, L. Dlháň, H. Fuess, A. Mašlejová, V. Mrázová, I. Svoboda, J. Titiš, *Polyhedron* **2006**, *25*, 3261–3268.
[24] P. Román, J. M. Gutierrez-Zorrilla, *J. Chem. Educ.* **1985**, *62*, 167.
[25] a) K. Nakamoto, *Infrared and Raman Spectra of Inorganic and Coordination Compounds*, 5th ed., John Wiley & Sons, New York, **1997**, part A, sect. II, pp. 153–321; b) R. L. Frost, K. L. Erikson, M. L. Weier, O. Carmody, *Spectrochim. Acta Part A* **2005**, *61*, 829–834.
[26] W. Yingua, *J. Appl. Crystallogr.* **1987**, *20*, 258–259.
[27] G. M. Sheldrick, *SHELXS97: Program for the Solution of Crystal Structures*, University of Göttingen, Göttingen, Germany, **1997**; G. M. Sheldrick, *Acta Crystallogr., Sect. A* **2008**, *64*, 112–122.
[28] G. M. Sheldrick, *SHELXL97: Program for the Refinement of Crystal Structures*, University of Göttingen, Göttingen, Germany, **1997**.
[29] *International Tables for X-ray Crystallography*, Kynoch Press, Birmingham, England, **1974**, vol. IV, p. 99.

Received: February 11, 2009
Published Online: July 14, 2009

